

IRAS LOW RESOLUTION SPECTRA OF ASTEROIDS

Russell G. Walker and Martin Cohen

Astronomy and Astrophysics

Vanguard Research, Inc.

Scotts Valley, California

Final Technical Report on Contract NASW-99025

April 16, 2002



Vanguard Research, Inc.
5321 Scotts Valley Drive
Suite 204
Scotts Valley, California 95066

UNCLASSIFIED

Abstract

Optical/near-infrared studies of asteroids are based on reflected sunlight and surface albedo variations create broad spectral features, suggestive of families of materials. There is a significant literature on these features, but there is very little work in the thermal infrared that directly probes the materials emitting on the surfaces of asteroids. We have searched for and extracted 534 thermal spectra of 245 asteroids from the original Dutch (Groningen) archive of spectra observed by the IRAS Low Resolution Spectrometer (LRS).

We find that, in general, the observed shapes of the spectral continua are inconsistent with that predicted by the standard thermal model used by IRAS (Lebofsky et al., 1986). Thermal models such as proposed by Harris (1998) and Harris et al.(1998) for the near-earth asteroids with the “beaming parameter” in the range of 1.0 to 1.2 best represent the observed spectral shapes. This implies that the IRAS Minor Planet Survey (IMPS, Tedesco, 1992) and the Supplementary IMPS (SIMPS, Tedesco, et al., 2002) derived asteroid diameters are systematically underestimated, and the albedos are overestimated.

We have tentatively identified several spectral features that appear to be diagnostic of at least families of materials. The variation of spectral features with taxonomic class hints that thermal infrared spectra can be a valuable tool for taxonomic classification of asteroids.

Table of Contents

Abstract	ii
List of Figures and Tables	iv
1. Introduction	1
2. Data Processing	2
3. Results	5
3.1 Thermal Models	5
3.2 Spectral Features	12
4. References	19

List of Figures and Tables

Figure 1a. Comparison of the observed IMPS declinations with those predicted by the LRS crossing program.	3
Figure 1b. Comparison of the observed IMPS right ascensions with predictions by the LRS crossing program.	3
Figure 2a. Comparison of observed IMPS declinations to the predicted orbital positions of the asteroids.	3
Figure 2b. Comparison of observed IMPS right ascensions to the predicted orbital positions of the asteroids.	3
Table 1. Distribution of LRS Spectra by Taxonomic Class.	5
Figure 3a. Co-added blue LRS spectra of 4 class C asteroids observed at high SNR. The asteroids are: 52 Europa, 45 Eugenia, 54 Alexandra, and 10 Hygeia.	6
Figure 3b. Co-added red LRS spectra of 4 class C asteroids observed at high SNR. The asteroids are: 52 Europa, 45 Eugenia, 54 Alexandra, and 10 Hygeia.	7
Figure 4a. Co-added blue LRS spectra of 2 class CP asteroids observed at high SNR. The asteroids are: 247 Eukrate and 694 Ekhard.	7
Figure 4b. Co-added red LRS spectra of 2 class CP asteroids observed at high SNR. The asteroids are: 247 Eukrate and 694 Ekhard.	8
Figure 5a. Co-added blue LRS spectra of the only class Gq asteroid observed, 1 Ceres.	8
Figure 5b. Co-added red LRS spectra of the only class Gq asteroid observed, 1 Ceres.	9
Figure 6a. Co-added blue LRS spectra of the only class S asteroid observed at high SNR, 3 Juno.	9

Figure 6b. Co-added red LRS spectra of the only class S asteroid observed at high SNR, 3 Juno.	10
Figure 7a. Co-added blue LRS spectra of both class m asteroids observed.	10
Figure 7b. Co-added red LRS spectra of three class m asteroids observed.	11
Figure 8a. Co-added blue LRS spectra of all class F asteroids observed.	11
Figure 8b. Co-added red LRS spectra of all class F asteroids observed.	12
Figure 9a. Comparison of co-added C spectra with high SNR members of the class.	13
Figure 9b. Comparison of co-added C spectra with high SNR members of the class.	13
Figure 10a. Comparison of co-added S spectra with a high SNR member of the class.	14
Figure 10b. Comparison of co-added S spectra with a high SNR member of the class.	14
Figure 11a. Comparison of co-added CP spectra with high SNR members of the class.	15
Figure 11b. Comparison of co-added CP spectra with high SNR members of the class.	15
Figure 12a. Co-added blue spectra of various taxonomic classes.	17
Figure 12b. Co-added red spectra of various taxonomic classes.	18

1. Introduction

Although asteroids are not the most primitive bodies in the solar system, we currently believe that they are planetismals that were never accreted into a major planet and thus not subject to extensive planetary formation processing. Collisional processes have altered the surface mineralogy of many asteroids. Still, others may be expected to have retained their pristine character and be indicators of physical conditions within the early solar system. For example: mineralogical variations correlated with distance from the Sun may give clues as to the temperature within the solar nebula at the distance where the asteroid was formed. It is well known (Gradie and Tedesco, 1982, Gradie et al, 1989) that the number density of S (silicate, high temperature) asteroids peaks at 2.2 au, while that of C (carbonaceous, low temperature) asteroids peaks at 3.0 au. Also, there is convincing evidence that most meteorites found on Earth had their origins in the asteroid belt.

Asteroids are dynamically characterized by their orbital elements and axial rotation, and physically characterized by their size and composition. Thermal emission from asteroids has been extensively used to estimate their diameters and albedos (Morrison, 1977, Morrison and Lebofsky, 1979), with the majority of these being derived from the IRAS observations (IMPS and SIMPS). IRAS also produced a valuable database of Low Resolution Spectra (LRS) of asteroids observed in the spectral region from 7.67 μm to 22.73 μm . These data have remained largely unanalyzed.

More recently, spectral features diagnostic of surface minerals have been identified in the thermal spectra of the Moon, Mercury, and a number of asteroids (see Sprague, 2000, Witteborn, et al., 2000). In the case of a dusty surface, these features can appear in either emission or absorption relative to the adopted continuum depending on the temperatures of the dust layer and the underlying surface. These features should be useful adjuncts to present taxonomic classification schemes, as well as, providing identification and verification of mineralogical composition.

Present taxonomic classification of asteroids relies on the observed albedo and reflection spectrum in the optical and near infrared (Tholen, 1984, Tholen, 1989, Tholen and Barucci, 1989, Tedesco, et al., 1989, Bus, 1999). There is a significant literature on the observed reflection features, but there is very little work in the thermal infrared that directly probes the materials emitting on the surfaces. In this paper we explore the thermal emission spectra of a large number of asteroids using the IRAS LRS database.

2. Data Processing

Our approach was to extract and recalibrate the LRS spectra; divide each spectrum by the best-fitting thermal continuum calculated from thermal models to enhance any spectral features (emission or absorption), and to remove the effects of heliocentric and geocentric distances and phase of the observation. The resulting spectrum we called the “emissivity” spectrum. We then co-added all the emissivity spectra of an individual asteroid. The final step was to co-add the emissivity spectra of individual asteroids by optical taxonomic class, and to search for any patterns of mid-infrared spectral features.

The field-of-view of the LRS spanned only $\frac{1}{2}$ the width of the IRAS focal plane array. A search was done on an IRAS scan-by-scan basis for each of the numbered asteroids using osculating orbital elements calculated for the 1983 epoch and provided to us by the Minor Planet Center. A total of 10666 asteroids were considered to have sufficiently good elements to be used in the search. An asteroid was selected from the list and its position computed for the time of the midpoint of the IRAS scan. If its position fell within the IRAS scan, the time that the scan crossed that position was found. Crossing times and positions were then iterated to closure. Parallax due to the orbiting spacecraft was included in the solution by interpolation of a time-ordered file of spacecraft heliocentric positions. Each asteroid was searched for its presence in all 5839 IRAS survey scans. As a check on the validity of the solution for the intersection we compared our crossing’s coordinates with those for 4167 sightings in common with the IMPS database. This is shown in Figure 1 for both right ascension and declination. Figure 2 shows the same statistics for the IMPS observed positions versus the asteroid positions predicted from the orbital elements. The differences are due to a combination of orbital prediction errors and IRAS positional uncertainties. Based on these plots a 1 arc minute search radius was used when searching the LRS database for matches.

Our initial search returned 35141 asteroid crossings, however, most of these were too faint to have been detected by the LRS. We estimated a reasonable upper limit to the flux from the asteroids in the IRAS 12 μm band at each “crossing” using the IRAS Standard Thermal Model (STM) with diameters estimated from the asteroid’s absolute magnitude. Using these estimates and a 20 Jy threshold at 12 μm , we found 1221 sightings for which extraction of usable LRS spectra seemed reasonable. The position and time of each sighting was input into software that searched the original Groningen archive of 171,000 extracted LRS spectra of point sources for a coordinate and time match. Spectra of 534 matches were automatically extracted and flux calibrated.

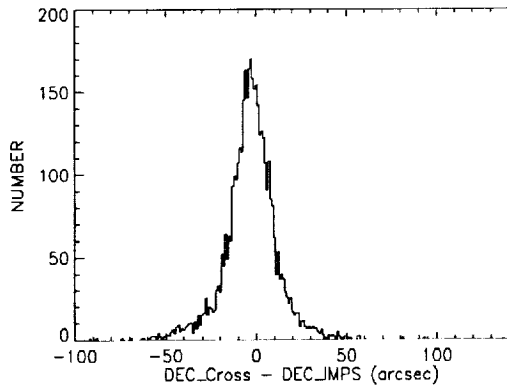


Figure 1a. Comparison of the observed IMPS declinations with those predicted by the LRS crossing program.

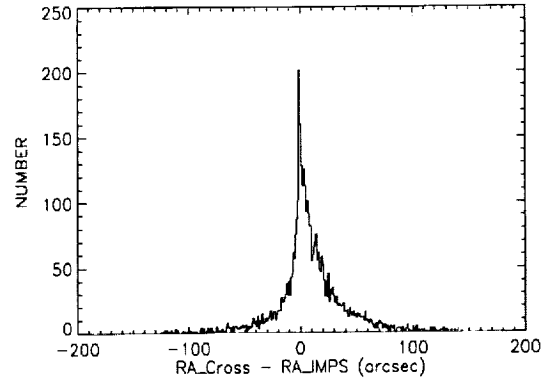


Figure 1b. Comparison of the observed IMPS right ascensions with predictions by the LRS crossing program.

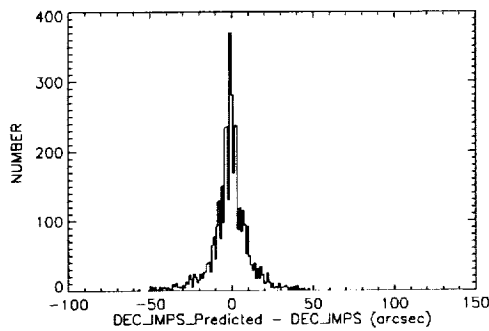


Figure 2a. Comparison of observed IMPS declinations to the predicted orbital positions of the asteroids.

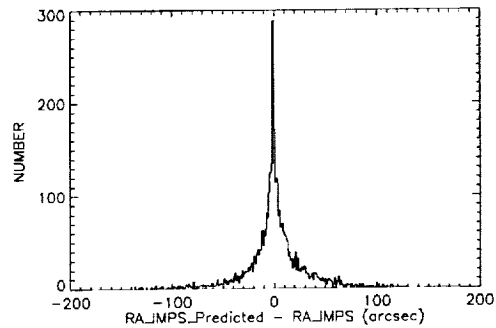


Figure 2b. Comparison of observed IMPS right ascensions to the predicted orbital positions of the asteroids.

The extracted LRS consists of 200 samples defining both a “blue” (7.6736 μ m to 13.446 μ m) spectrum and a “red” (10.607 μ m to 22.737 μ m) spectrum measured with separate prism spectrometers. The blue spectrum consists of 44 samples of the spectral irradiance at roughly equal wavelength intervals followed by 19 samples of “dark” response that is useful for noise and baseline determination. Similarly the red spectrum consists of 49 samples of the spectrum followed by 19 samples of the “dark” response.

Our processing began by separating the two spectra and calculating the noise for each. The noise consisted of two components: a constant value calculated from the dark

response and a response dependent component (approximately 1% of the irradiance) due to the encoding algorithm used on the satellite. The calculated noise was the basis for all error bars subsequently developed. Once the noise had been calculated, an estimate of the median signal to noise ratio (SNR) in the spectrum was then calculated. This was defined as: $SNR = \text{median}(\text{irradiance smoothed with a 9-point boxcar}) / \text{median}(\text{noise})$. Spectra with $SNR < 3.0$ were rejected from further consideration. This was based upon our previous experience that such spectra usually proved unreliable and could adversely effect subsequent co-additions. This severe test rejected 376 blue and 307 red spectra.

We maintained the blue and red spectra separate throughout the data processing and analysis rather than splice them into a single spectrum as is customary for LRS. Information in the overlap region is usually degraded due to the process of combining two spectra of different resolving powers. We preferred to use the overlap region (10.607 μm to 13.446 μm) to self-confirm any spectral features seen within the region.

Most asteroids in our data set were observed two or more times, and thus at two or more heliocentric and geocentric distances and phase angles. The thermal continuum that is dependent upon these geometrical parameters must be removed from the spectrum prior to co-adding (averaging) these spectra to optimize the detection of spectral features that are intrinsic to the asteroid. Dividing the LRS by a spectrum calculated using the Standard Thermal Model and the asteroid's albedo and diameter from the IMPS (Tedesco, 1992) database accomplished this. The resulting emissivity spectrum was then normalized such that the median emissivity was unity. This was done to minimize the effects of errors in the IMPS diameters and in the absolute calibration of the LRS.

The next step was to co-add with inverse variance weighting the multiple spectra of each asteroid to produce a single blue and red spectrum for each asteroid. This was done in an interactive program where each spectrum could be visually evaluated prior to co-addition. An editing tool was used to assign low weights to fluxes that were single event "glitches" (most likely due to high-energy particle events). Entire spectra were rejected if they were clearly discrepant upon examination (1 red and 3 blue spectra were rejected on this criterion).

The final step in the processing was to co-add the spectra within a common taxonomic class. The taxonomic classification scheme adopted was that of Tedesco, et al. (1989) where available and Tholen (1989) to fill in missing classifications. The co-addition was done with visual display but no interactive capability. Table 1 shows the resulting distribution with taxonomic class of those asteroids having an LRS. The final selection contains 75 asteroids with 155 LRS and 101 asteroids with 226 LRS. The greatest number is in the C and S classes as might have been expected, with CP being the next most populous.

Taxonomic Class	LRS Blue Spectra		LRS Red Spectra	
	Number of Asteroids	Number of LRS	Number of Asteroids	Number of LRS
BF	1	3	1	3
C	27	54	40	78
CF	0	0	1	1
CG	0	0	1	1
CP	8	17	8	18
Cq	1	5	2	7
CU	0	0	1	3
CX	3	7	3	7
DP	1	1	1	2
F	2	7	3	9
FC	0	0	1	1
G	2	3	2	4
Gq	1	3	1	2
l	3	5	2	5
m	2	7	3	10
PC	1	2	3	9
r	1	1	2	3
S	20	37	21	57
T	1	2	2	3
TD	0	0	1	1
X	0	0	1	1
Unclassified	1	1	1	1
Total	75	155	101	226

3. Results

3.1 Thermal Models

Our expectation was that an emissivity spectrum with mean slope of zero would result from the above process using the IRAS STM (Lebofsky, et al, 1986). This was indeed not the case. In fact, we found only 1 asteroid (344 Desiderata) for which this was true. For all other individual asteroids and classes the IRAS STM produced spectra that were too blue, that is, representative of a higher surface temperature distribution than is consistent with the observations. This is similar to that noted by Harris (1998) and Harris, et al. (1998) for the near-Earth asteroids (NEA). Harris proposed a near-Earth thermal model (NEATM). The NEATM integrates the Lambertian emission over the

surface of the planet at the phase observed, rather than assuming a fixed phase coefficient of 0.01 mag/degree; and allows the “beaming” parameter, β , to be varied to give a best fit to the observed spectral distribution. He found that $\beta > 1.0$ was required to fit the NEA energy distribution as opposed to $\beta = 0.756$ used in the STM.

At this point we decided to investigate the behavior of the emissivity spectra for different choices of η using the NEATM. Figures 3a thru 6b are plots of emissivity spectra of individual asteroids or classes of asteroids that were observed at high SNR. The plots compare the spectra for three choices of $\beta = 0.756$, $\beta = 1.0$ and $\beta = 1.2$. The error bars have been suppressed on these plots for clarity. We are not concerned about the structure here, but rather the mean slope of the spectrum, and, of course, we desire a single continuum to fit both the blue and red spectra. It is clear that $\beta = 0.756$ does not reproduce the shape of the continuum for any of the classes shown. Classes C, S, and Gq are better reproduced with $\beta = 1$, while $\beta = 1.2$ is a good choice for Class CP. Figures 7 and 8 show the spectra for Classes F and m. These were observed at lower SNR and the choice of β is not quite so clear, however, $\beta = 1.0$ still appears to give a better fit to the continuum than $\beta = 0.756$.

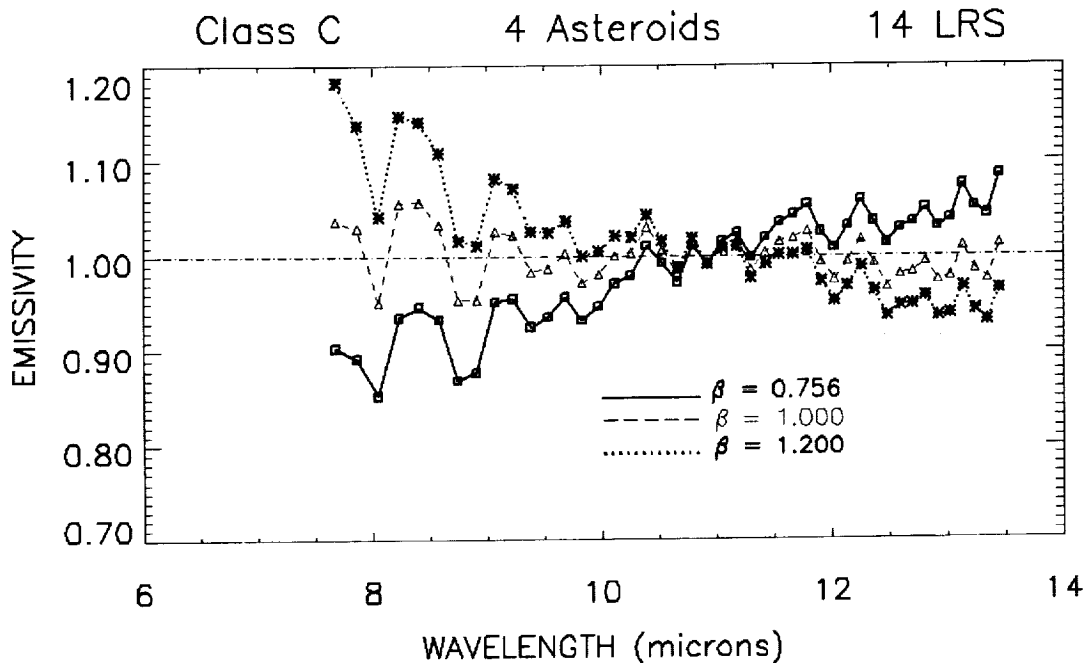


Figure 3a. Coadded blue LRS spectra of 4 class C asteroids observed at high SNR. The asteroids are: 52 Europa, 45 Eugenia, 54 Alexandra, and 10 Hygeia.

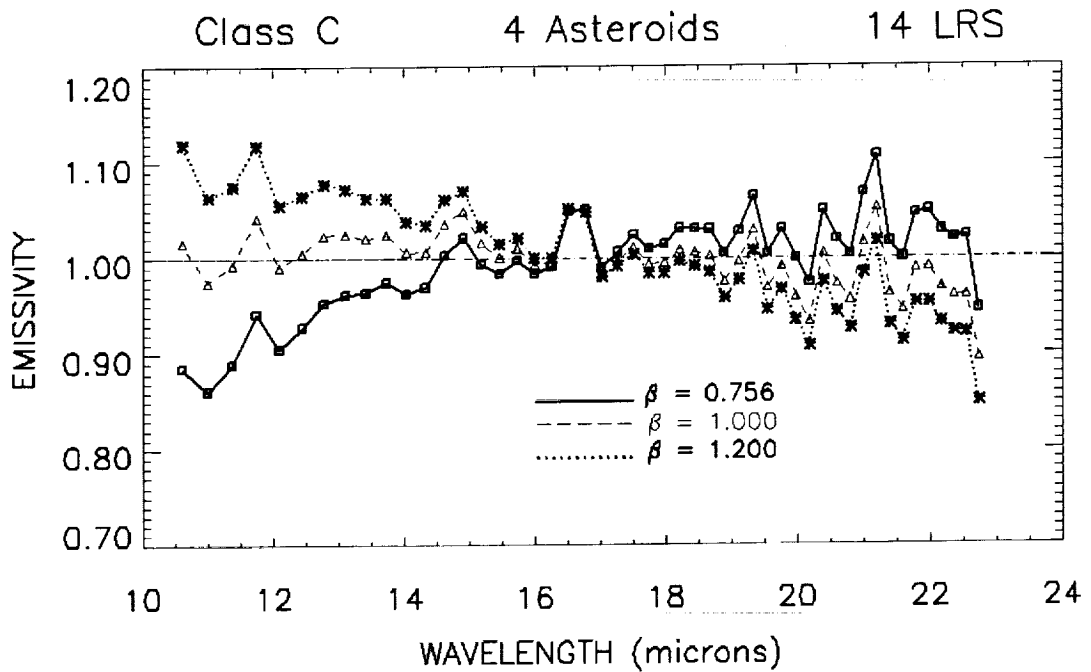


Figure 3b. Coadded red LRS spectra of 4 class C asteroids observed at high SNR. The asteroids are: 52 Europa, 45 Eugenia, 54 Alexandra, and 10 Hygeia.

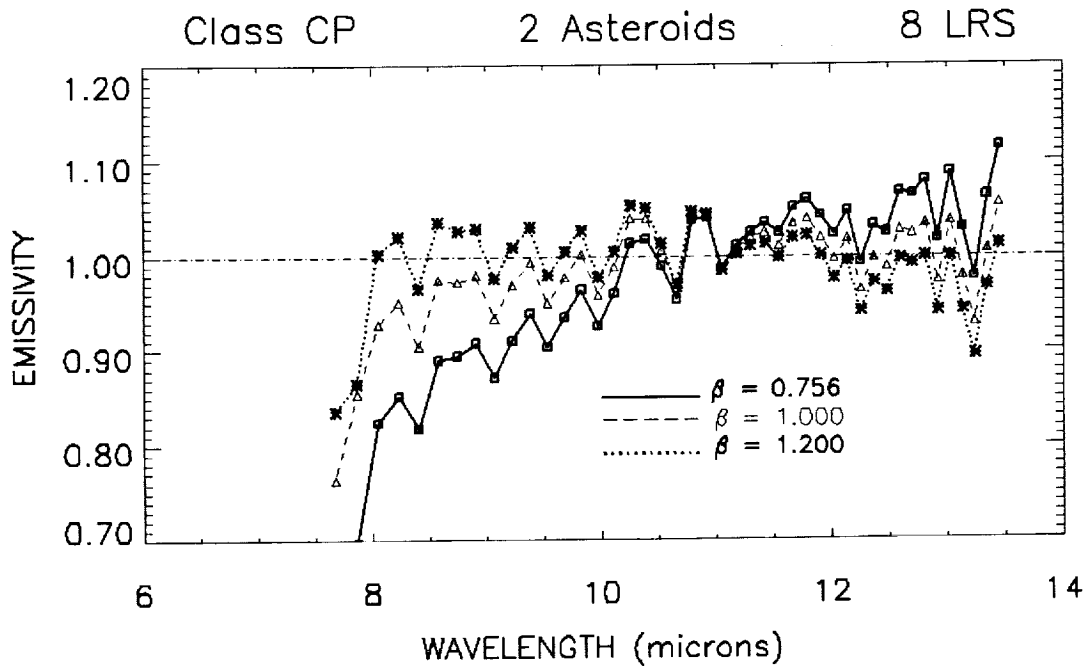


Figure 4a. Coadded blue LRS spectra of 2 class CP asteroids observed at high SNR. The asteroids are: 247 Eukrate and 694 Ekhard.

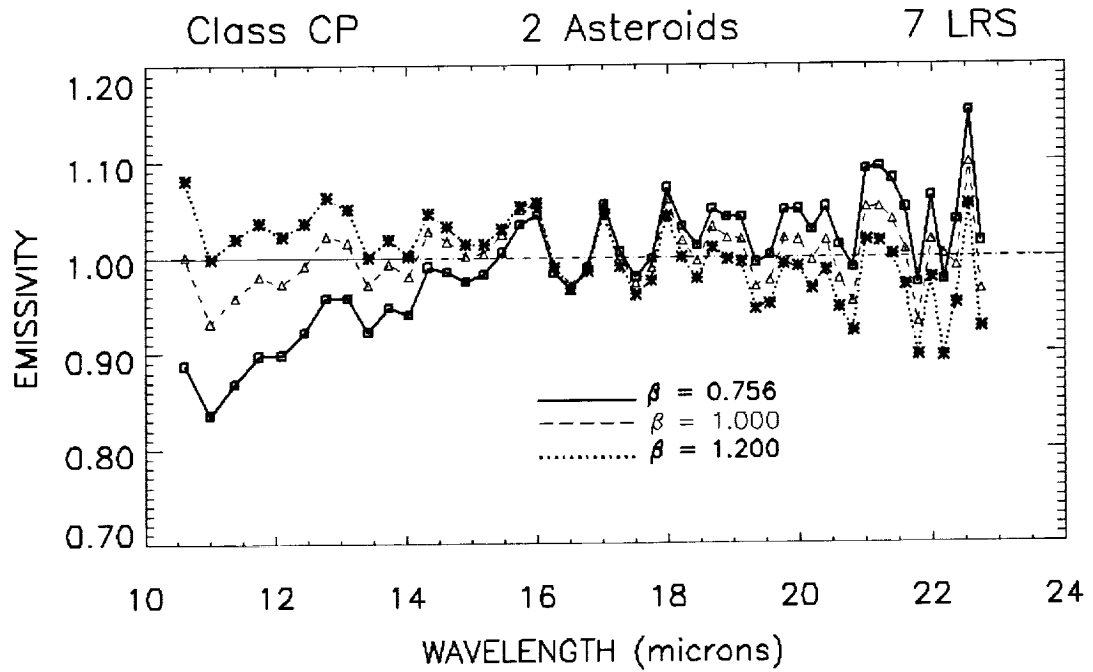


Figure 4b. Coadded red LRS spectra of 2 class CP asteroids observed at high SNR. The asteroids are: 247 Eukrate and 694 Ekhard.

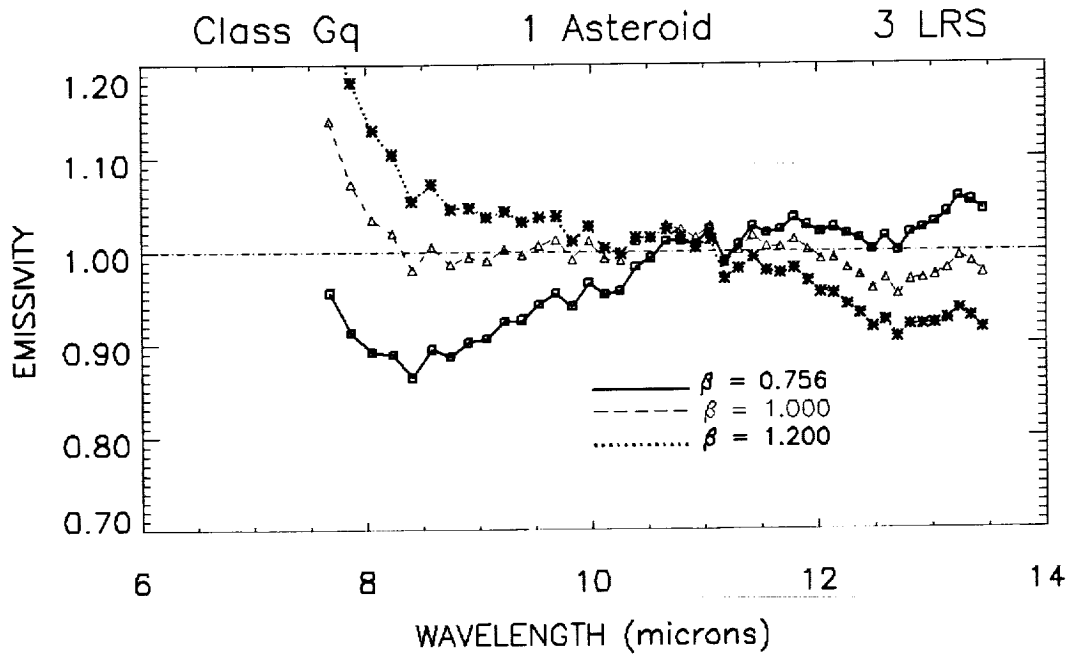


Figure 5a. Coadded blue LRS spectra of the only class Gq asteroid observed, 1 Ceres.

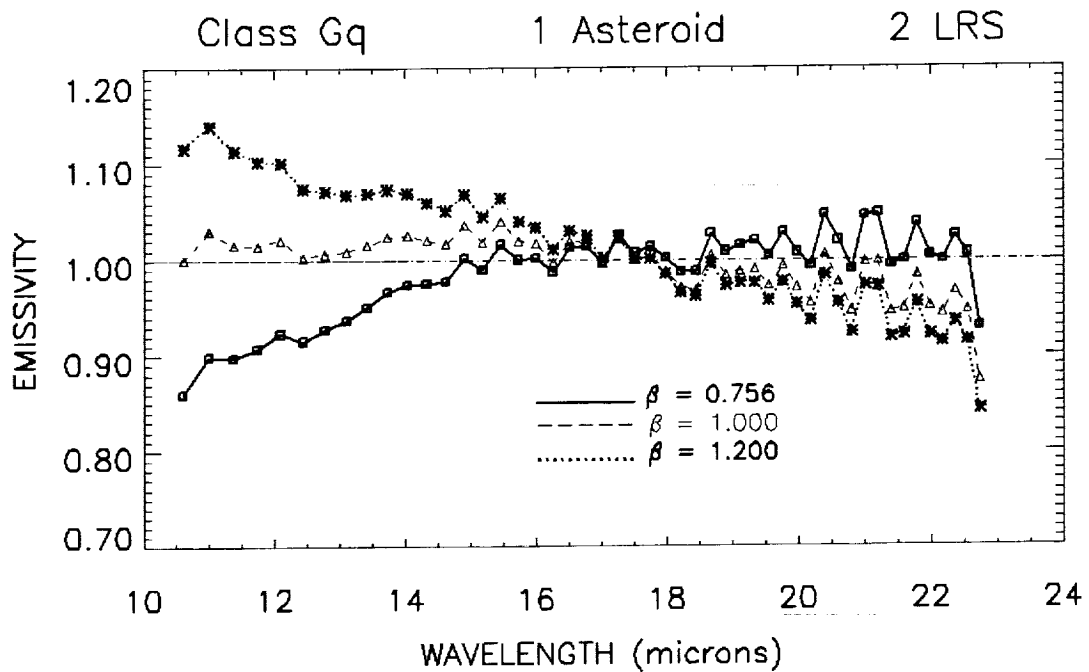


Figure 5b. Coadded red LRS spectra of the only class Gq asteroid observed, 1 Ceres.

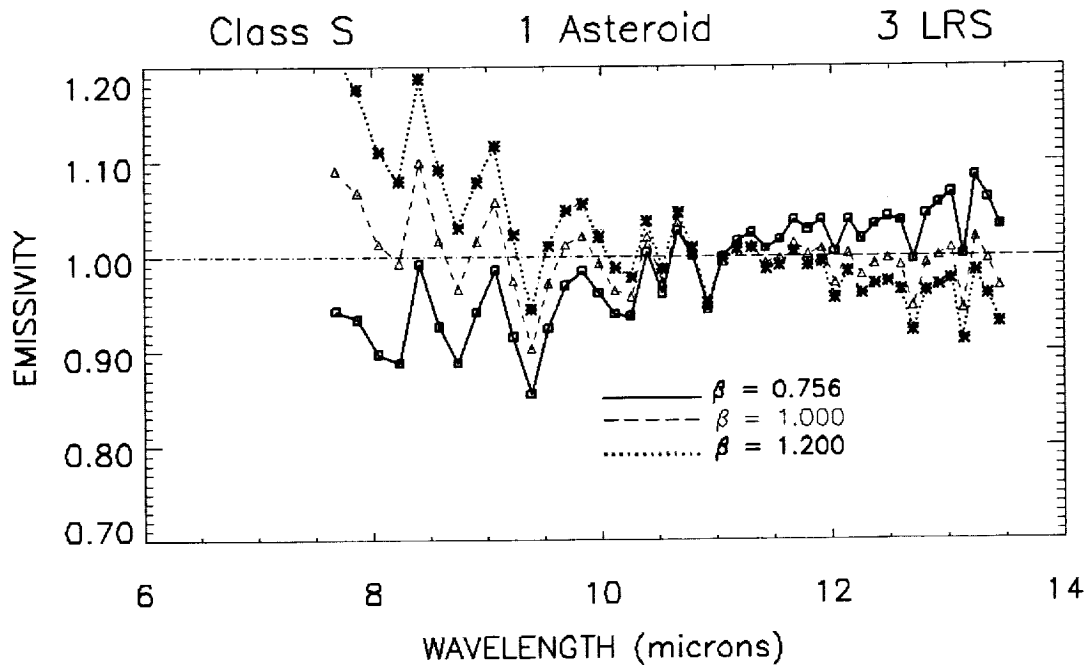


Figure 6a. Coadded blue LRS spectra of the only class S asteroid observed at high SNR, 3 Juno.

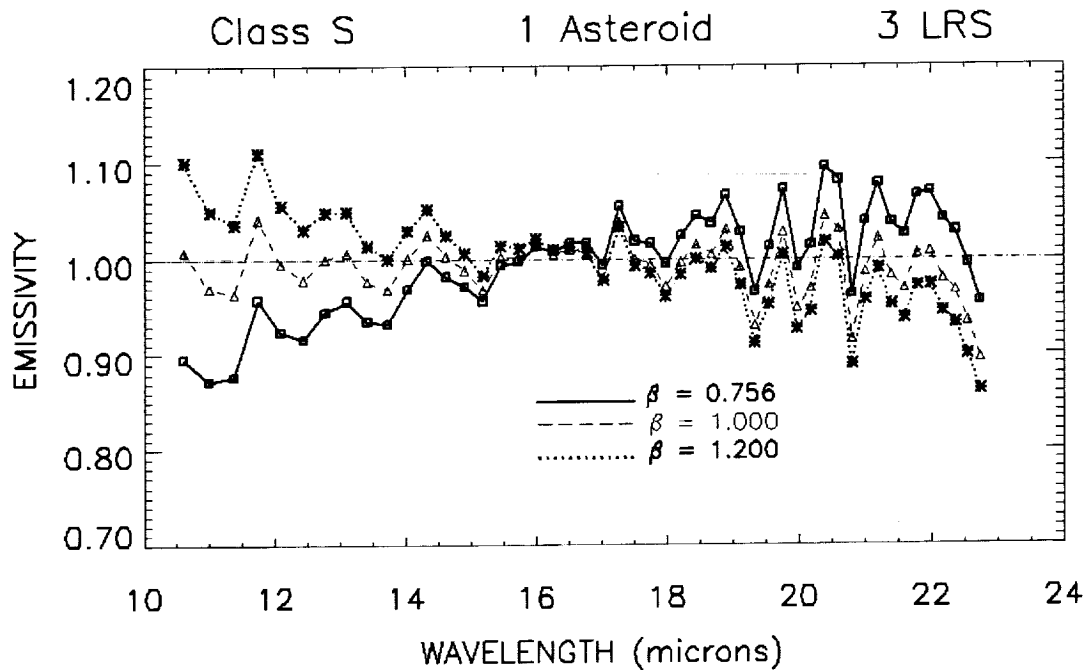


Figure 6b. Coadded red LRS spectra of the only class S asteroid observed at high SNR, 3 Juno.

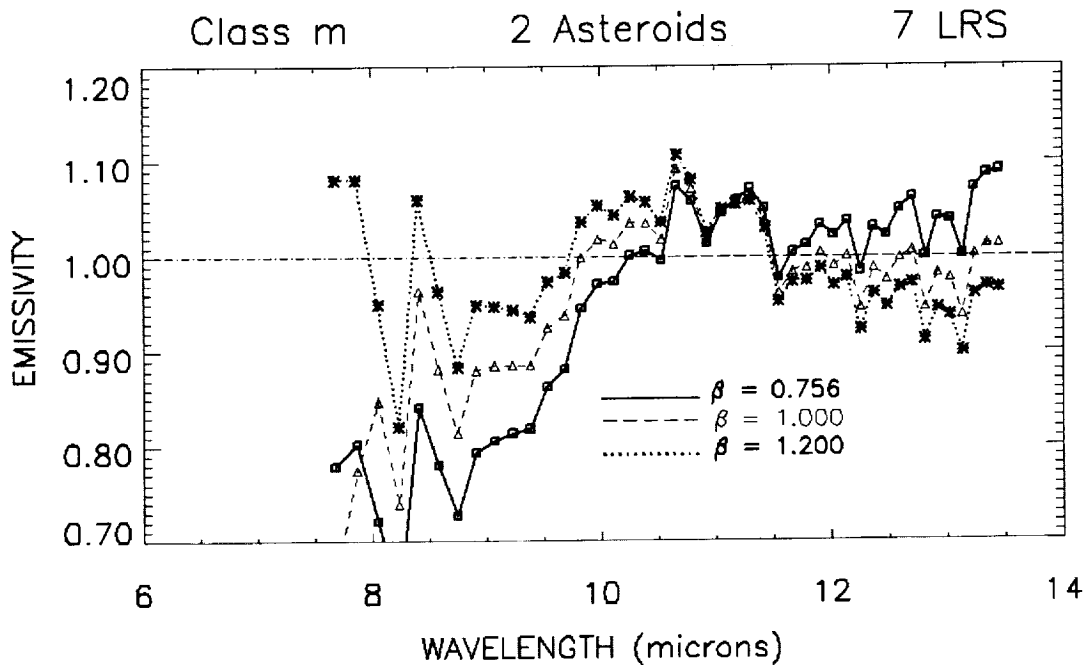


Figure 7a. Coadded blue LRS spectra of both class m asteroids observed.

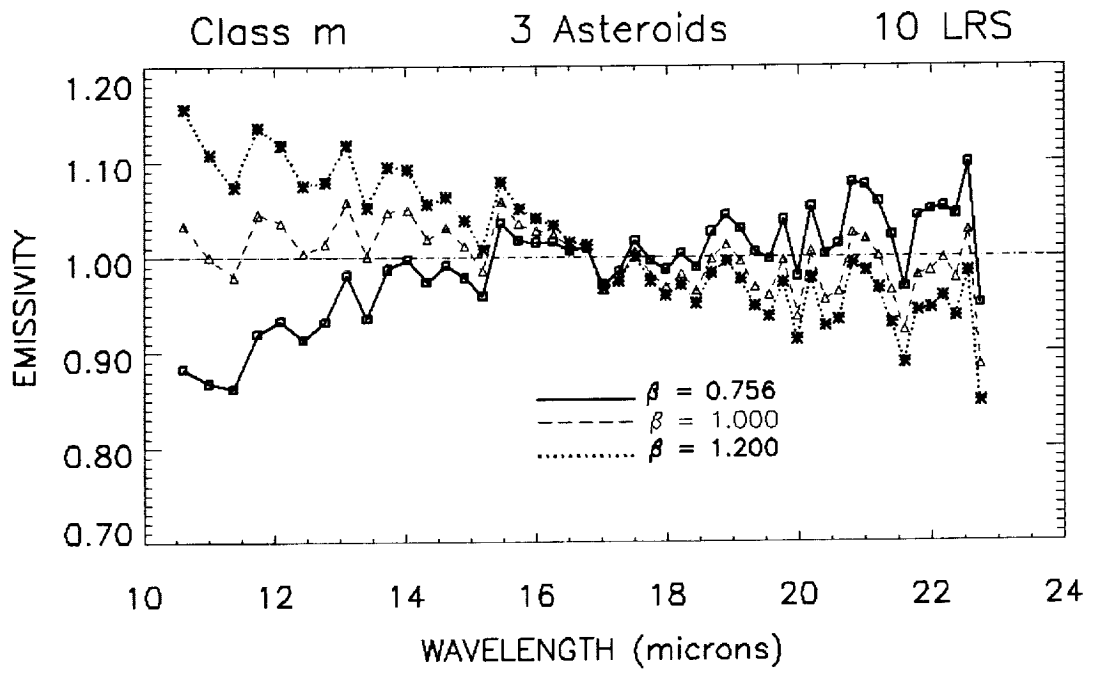


Figure 7b. Coadded red LRS spectra of three class m asteroids observed.

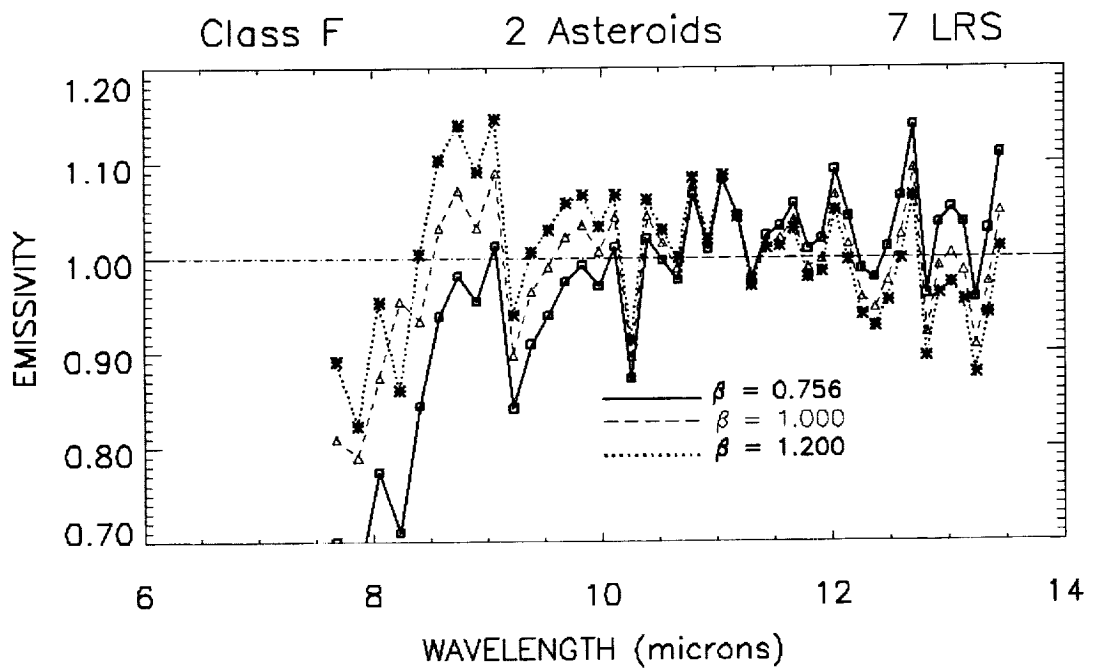


Figure 8a. Coadded blue LRS spectra of all class F asteroids observed.

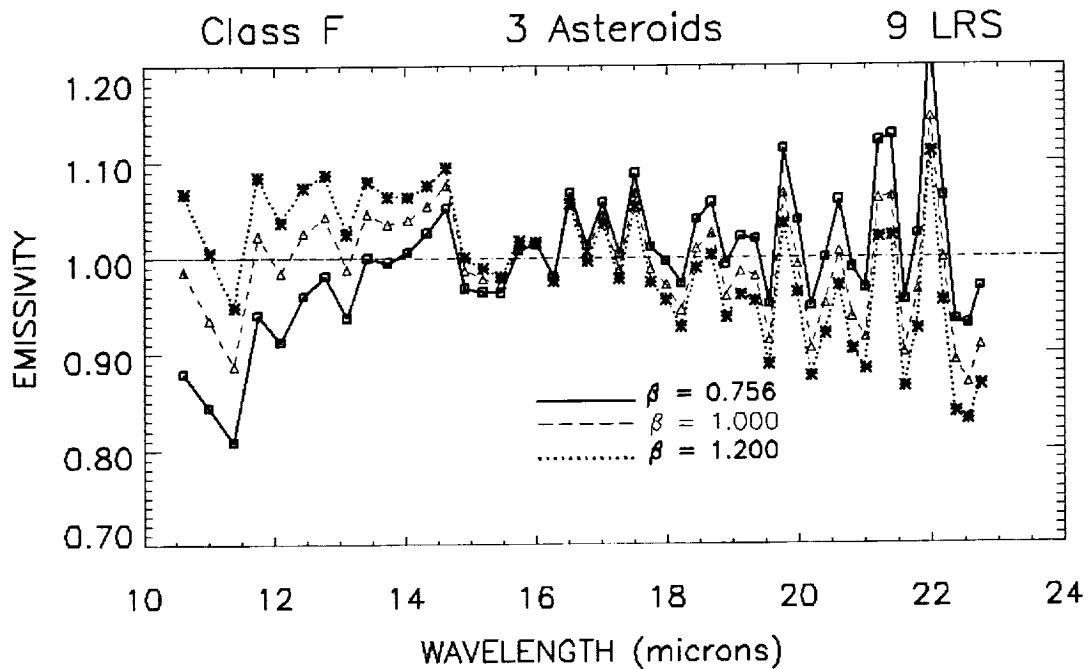


Figure 8b. Coadded red LRS spectra of all class F asteroids observed.

It seems clear that the thermal continuum spectrum of asteroids is not well represented by the IRAS STM with $\beta = 0.756$ and, in general, the thermal spectrum is better represented by the NEATM approach with $\beta \geq 1.0$, even for main belt asteroids. This implies that diameters derived using the IRAS STM are systematically underestimated and the associated albedos overestimated. The magnitudes of the diameter and albedo errors are probably dependent on the taxonomic class of the asteroid.

3.2 Spectral Features

The question of definitive spectral features and their relation to asteroid surface mineralogy is a complex one. Figures 9a thru 11b compare the brighter members of a class to the co-addition of the fainter class members (the bright members being excluded from the co-add). The error bars are 1 sigma. It is easily seen in Figure 9 that several features in 54 Alexandra and 45 Europa are seen in 10 Hygiea. These are also present in the co-added C-class spectrum. Similarly, in Figure 10 we see features in the spectrum of 3 Juno that are mimicked in the co-added S-class spectrum. Figure 11 compares spectra of class CP.

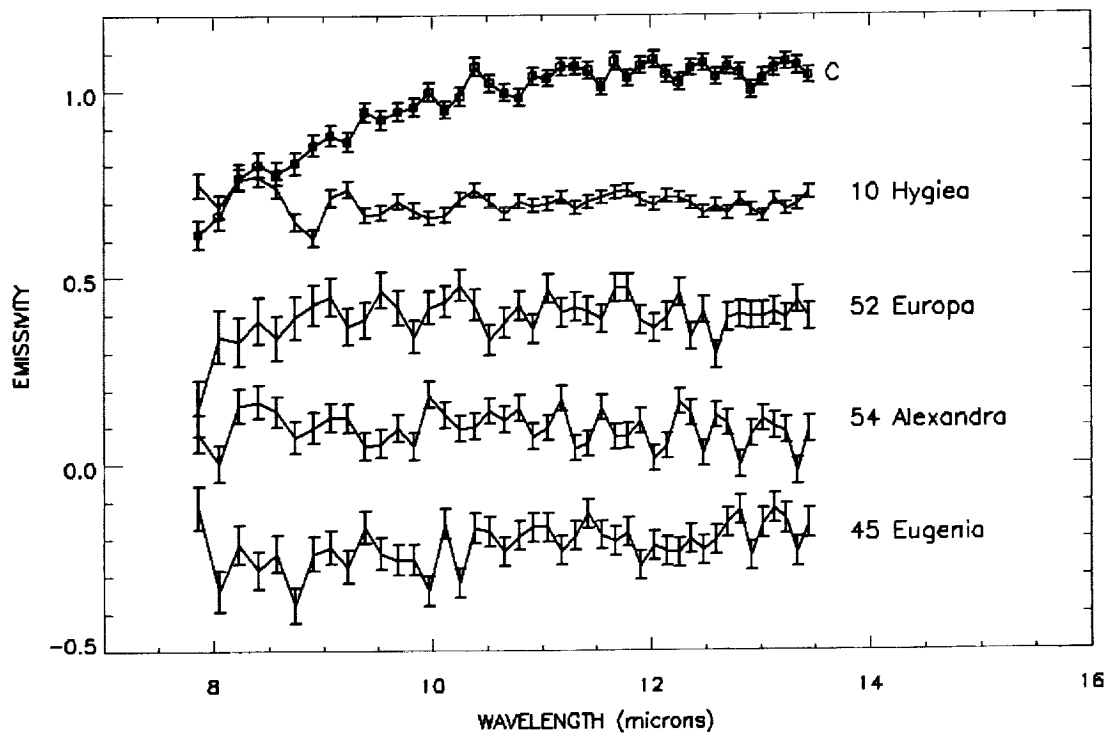


Figure 9a. Comparison of co-added C spectra with high SNR members of the class.

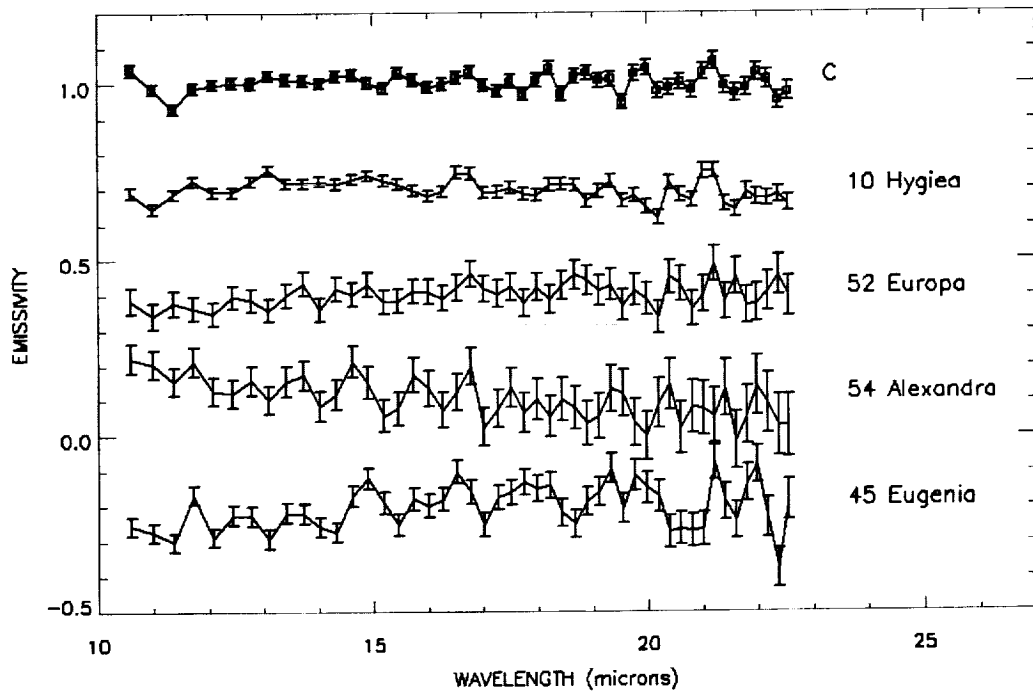


Figure 9b. Comparison of co-added C spectra with high SNR members of the class.

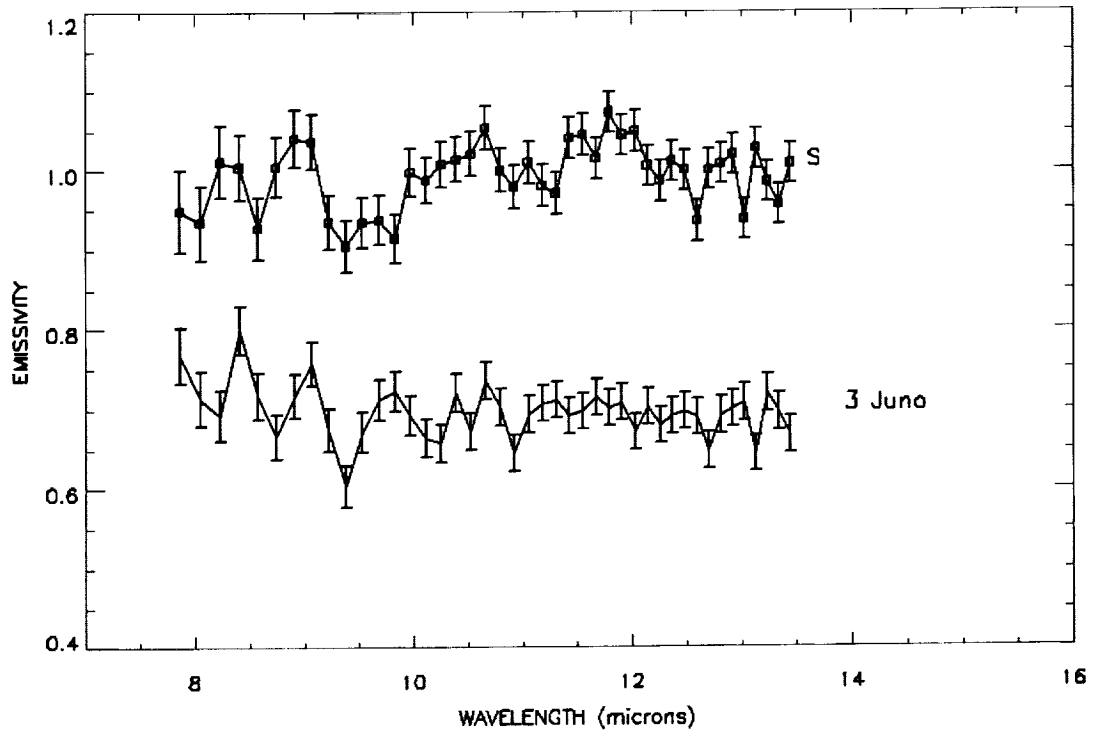


Figure 10a. Comparison of co-added S spectra with a high SNR member of the class.

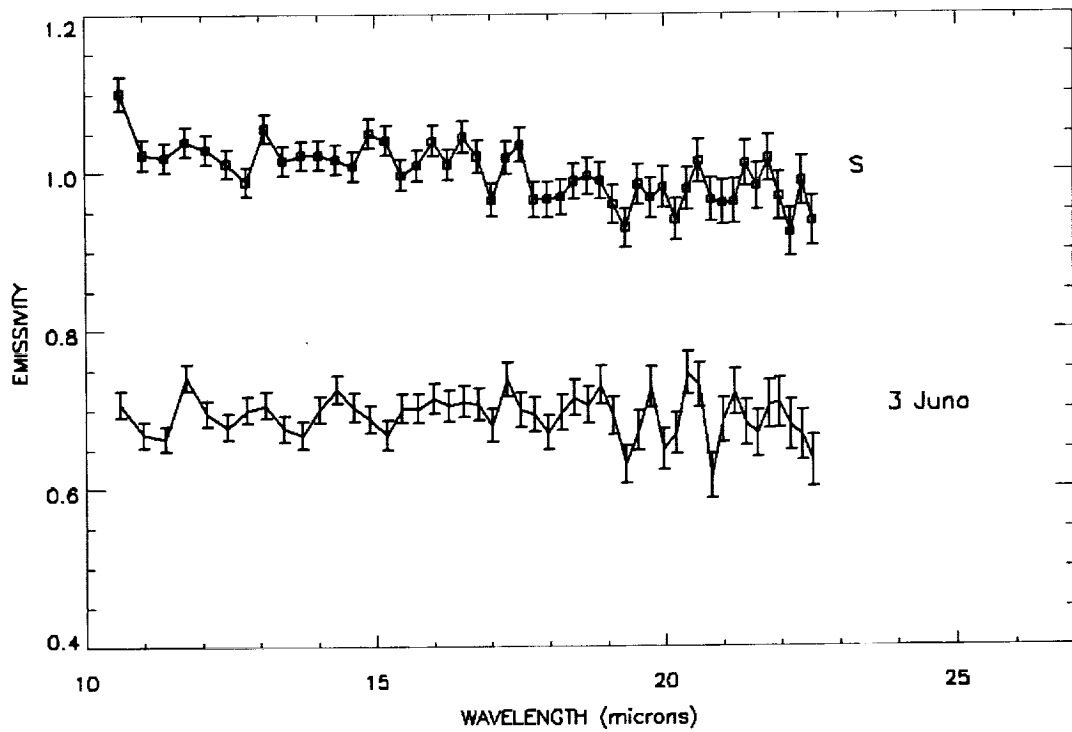


Figure 10b. Comparison of co-added S spectra with a high SNR member of the class.

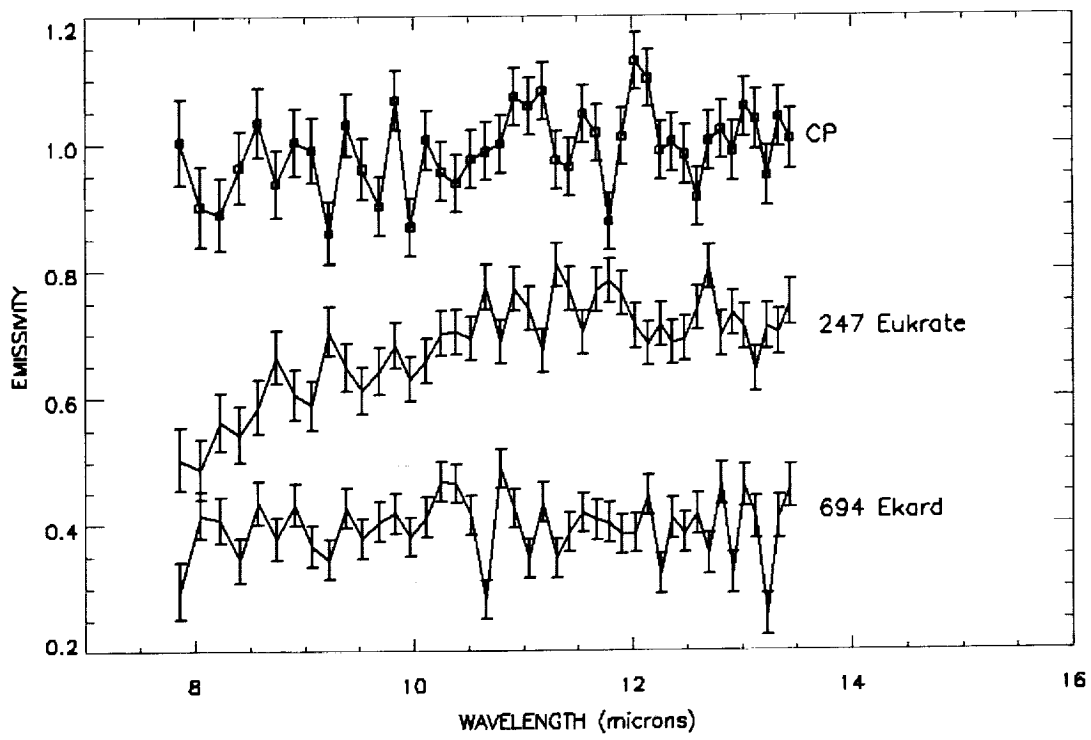


Figure 11a. Comparison of co-added CP spectra with high SNR members of the class.

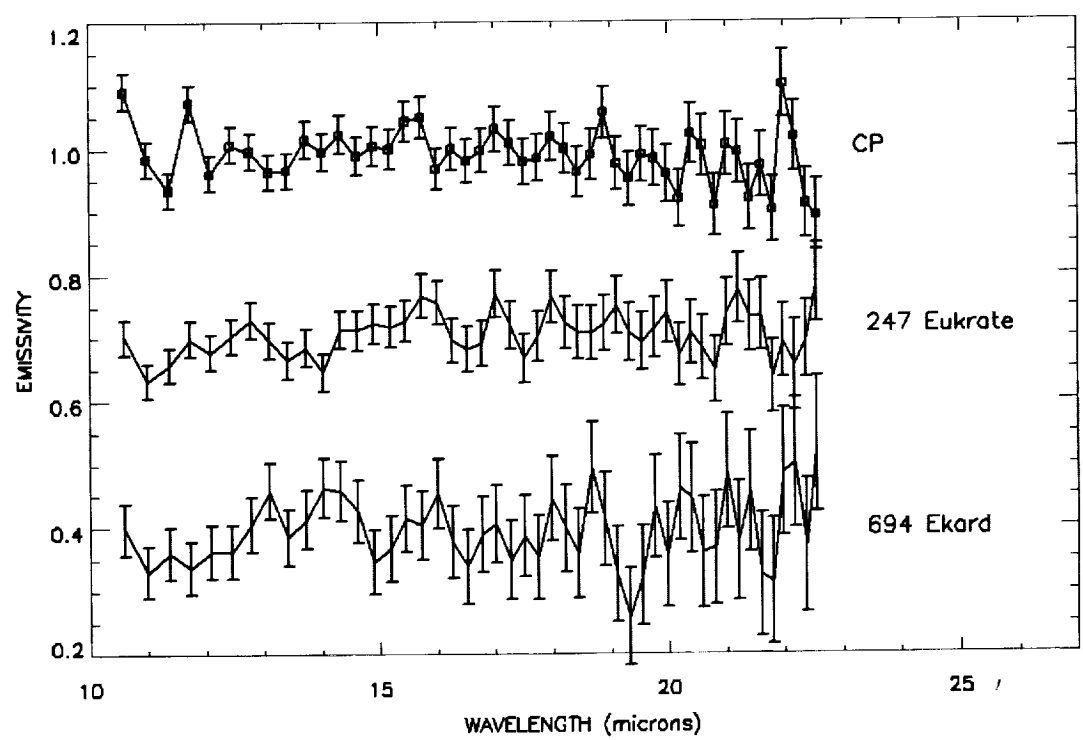


Figure 11b. Comparison of co-added CP spectra with high SNR members of the class.

It is clear that we are still in the realm of low SNR in most cases, making positive detection and identification of features difficult. A further complication arises from the viewing geometry. Spectral features that appear in emission on the evening hemisphere may appear in absorption on the morning hemisphere, while they may disappear in pole-on observations. Further analysis must account for this effect.

Figures 12a, b are composites of all the taxonomic types that were observed. Poor SNR dominates most of these spectra rendering taxonomic variations uncertain. These data will be reexamined taking account of asteroid rotation (morning-evening variations) and reduced to the new taxonomic system proposed by Bus (1999). A paper is in preparation for submission to the journal ICARUS.

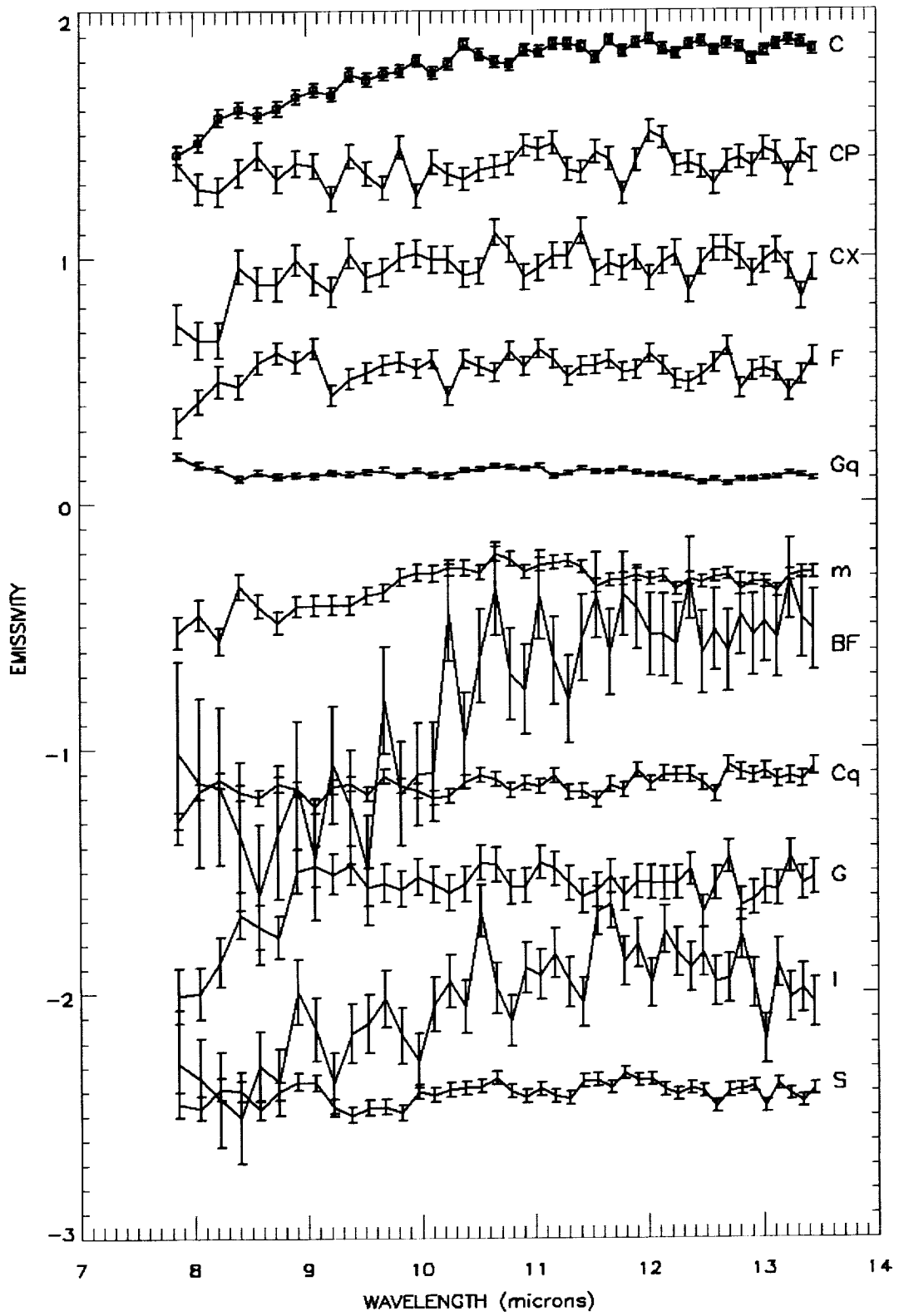


Figure 12a. Co-added blue spectra of various taxonomic classes.

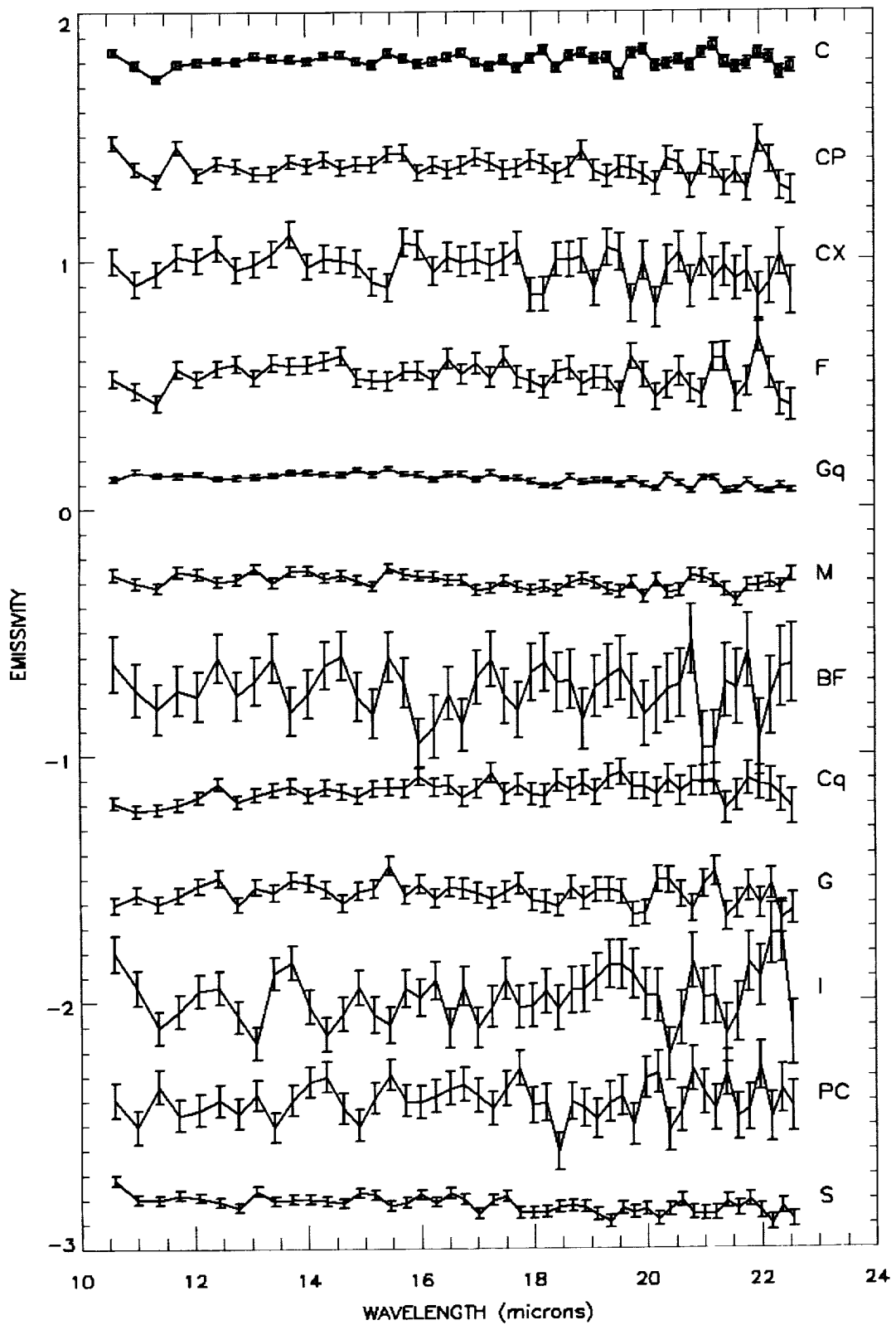


Figure 12b. Co-added red spectra of various taxonomic classes.

4. References

- Bus, S.J., 1999, *Compositional Structure in the Asteroid Belt: Results of a Spectroscopic Survey*, Doctoral Thesis, Mass. Inst. of Tech.
- Gradie, J.C. and Tedesco, E.F., 1982, *Science*, **216**, 1405-1407
- Gradie, J.C., Chapman, C.R., and Tedesco, E.F., 1989, In *Asteroids II* (R.P. Binzel, T. Gehrels, M.S. Mathews, Eds.), pp 316-335, Univ. of Arizona Press, Tucson
- Harris, A.W., 1998, *ICARUS*, **131**, 291-301
- Harris, A.W., Davies, J.K., and Green, S.F., 1998, *ICARUS*, **135**, 441-450
- Lebofsky, L.A., Sykes, M.V., Tedesco, E.F., Veeder, G.J., Matson, D.L., Brown, R.H., Gradie, J.C., Feierberg, M.A., and Rudy, R.J., 1986, *ICARUS*, **68**, 239-251
- Morrison, D., 1977, *Astrophys. J.*, **214**, 667-677
- Morrison, D. and Lebofsky, L.A., 1979, In *Asteroids*, (T.Gehrels, Ed.) pp. 184-205, Univ. of Arizona Press, Tucson
- Sprague, A.L., 2000, *Thermal Emission Spectroscopy and Analysis of Dust, Disks, and Regoliths*, ASP Conference Series, **196**, pp167-186
- Tedesco, E.F., Williams, J.G., Matson, D.L., Veeder, J.G., Gradie, J.C., and Lebofsky, L.A., 1989, In *Asteroids II* (R.P. Binzel, T. Gehrels, M.S. Mathews, Eds.), pp 1151-1161, Univ. of Arizona Press, Tucson
- Tedesco, E.F., 1992, *IRAS Minor Planet Survey (IMPS)*, Phillips Laboratory, Technical Report No. PL-TR-92-2049. Hanscom Air Force Base, MA
- Tedesco, E.F., Noah, P.V., Noah, M., and Price, S.D., 2002, *Astron. J.*, **123**, 1056-1085
- Tholen, D.J., 1984, *Asteroid Taxonomy From Cluster Analysis Of Photometry*, Doctoral Thesis, Univ. of Arizona
- Tholen, D.J., 1989, In *Asteroids II* (R.P. Binzel, T. Gehrels, M.S. Mathews, Eds.), pp 1139-1150, Univ. of Arizona Press, Tucson
- Tholen, D.J. and Barucci, M.A., 1989, In *Asteroids II* (R.P. Binzel, T. Gehrels, M.S. Mathews, Eds.), pp 298-315, Univ. of Arizona Press, Tucson
- Witteborn, F.C., Roush, T.L., and Cohen, M., 2000, *Thermal Emission Spectroscopy of 1 Ceres: Evidence for Olivine*, ASP Conference Series, **196**, pp197-203

REPORT DOCUMENTATION PAGE

Form Approved
OMB No. 0704-0188

Public reporting burden for this collection of information is estimated to average 1 hour per response, including the time for reviewing instructions, searching existing data sources, gathering and maintaining the data needed, and completing and reviewing the collection of information. Send comments regarding this burden estimate or any other aspect of this collection of information, including suggestions for reducing this burden, to Washington Headquarters Services, Directorate for Information Operations and Reports, 1215 Jefferson Davis Highway, Suite 1204, Arlington, VA 22202-4302, and to the Office of Management and Budget, Paperwork Reduction Project (0704-0188), Washington, DC 20503.

1. AGENCY USE ONLY (Leave blank)	2. REPORT DATE April 16, 2002	3. REPORT TYPE AND DATES COVERED Final Report	
4. TITLE AND SUBTITLE IRAS Low-Resolution Spectra of Asteroids		5. FUNDING NUMBERS NASW-99025	
6. AUTHORS Martin Cohen and Russell G. Walker		8. PERFORMING ORGANIZATION REPORT NUMBER VRISV 1140-001-Final Report	
7. PERFORMING ORGANIZATION NAME(S) AND ADDRESS(ES) Vanguard Research, Inc. 5321 Scotts Valley Drive, Suite 204 Scotts Valley, CA 95066		10. SPONSORING/MONITORING AGENCY REPORT NUMBER	
9. SPONSORING/MONITORING AGENCY NAME(S) AND ADDRESS(ES) NASA Goddard Space Flight Center Headquarters Procurement Office, CODE 210.H Greenbelt, MD 20771		11. SUPPLEMENTARY NOTES	
12a. DISTRIBUTION/AVAILABILITY STATEMENT Approved for Public Release; Distributed Unlimited.		12b. DISTRIBUTION CODE	
<p>13. ABSTRACT (Maximum 200 words) Optical/near-infrared studies of asteroids are based on reflected sunlight and surface albedo variations create broad spectral features, suggestive of families of materials. There is a significant literature on these features, but there is very little work in the thermal infrared that directly probes the materials emitting on the surfaces of asteroids. We have searched for and extracted 534 thermal spectra of 245 asteroids from the original Dutch (Groningen) archive of spectra observed by the IRAS Low Resolution Spectrometer (LRS).</p> <p>We find that, in general, the observed shapes of the spectral continua are inconsistent with that predicted by the standard thermal model used by IRAS (Lebofsky et al., 1986). Thermal models such as proposed by Harris (1998) and Harris et al.(1998) for the near-earth asteroids with the "beaming parameter" in the range of 1.0 to 1.2 best represent the observed spectral shapes. This implies that the IRAS Minor Planet Survey (IMPS, Tedesco, 1992) and the Supplementary IMPS (SIMPS, Tedesco, et al., 2002) derived asteroid diameters are systematically underestimated, and the albedos are overestimated.</p> <p>We have tentatively identified several spectral features that appear to be diagnostic of at least families of materials. The variation of spectral features with taxonomic class hints that thermal infrared spectra can be a valuable tool for taxonomic classification of asteroids.</p>			
14. SUBJECT TERMS infrared, asteroids, spectra		15. NUMBER OF PAGES 19	16. PRICE CODE
17. SECURITY CLASSIFICATION OF REPORT UNCLASSIFIED	18. SECURITY CLASSIFICATION OF THIS PAGE UNCLASSIFIED	19. SECURITY CLASSIFICATION OF ABSTRACT UNCLASSIFIED	20. LIMITATION OF ABSTRACT UL